Supporting Information

Femtosecond Conical Intersection Dynamics of Tryptophan in Proteins and Validation of Slowdown of Hydration Layer Dynamics

Jin Yang,† Luyuan Zhang,† Lijuan Wang and Dongping Zhong*

Department of Physics, Department of Chemistry and Biochemistry, and Programs of Biophysics, Chemical Physics, and Biochemistry, The Ohio State University, Columbus, OH 43210, United States

Data Analysis

Upon 290-nm fs-pulse excitation, the two nearly degenerate states, ^1L_a and ^1L_b, will be excited coherently as a superposition state: $|\Psi\rangle = \sqrt{n_a^*}|a\rangle + \sqrt{n_b^*}|b\rangle$, where n_a^* and n_b^* are the relative probabilities of the ^1L_a and ^1L_b states, respectively, and $n_a^* + n_b^* = 1$.

Depending on how the coherence dephasing process and internal conversion dynamics evolve, various models could be proposed. Here, we assume that these two processes proceed in a parallel or sequential way, and build two corresponding models to simulate our experimental data. A detailed description of the two models is given as follows.

(1) Sequential model

In this model, we assumed that the population of the superposition state, $n_c(t)$, decays into the ^1L_a and ^1L_b states with a dephasing time T_2. After dephasing, the system can be treated with the mixed populations of the ^1L_a, $n_a(t)$, and ^1L_b, $n_b(t)$, states. As the fluorescence emission from the ^1L_a state follows a multiple exponential decay due to solvation when gated at a certain wavelength (for example, 310 nm or 335 nm), the time-dependent populations of the three states can be written as:

$$n_c(t) = e^{-t/T_2} = c(t) \tag{S1}$$

$$n_a(t) = n_a^* \sum_i a_i \frac{\tau_i}{\tau_i - T_2}(e^{-t/\tau_i} - e^{-t/T_2}) = n_a^* a(t), \ \sum_i a_i = 1 \tag{S2}$$

$$n_b(t) = n_b^* \frac{\tau_{IC}}{\tau_{IC} - T_2}(e^{-t/\tau_{IC}} - e^{-t/T_2}) = n_b^* b(t) \tag{S3}$$

For molecules that are initially excited in the ^1L_b state and then transferred to the ^1L_a state via conical intersection, the population is named $n_{ba}(t)$ as follows,

$$n_{ba}(t) = n_b^* \sum_i a_i [\frac{\tau_i}{\tau_{IC} - T_2}(\frac{\tau_{IC}}{\tau_{IC} - \tau_i} e^{-t/\tau_{IC}} - \frac{T_2}{T_2 - \tau_i} e^{-t/T_2}) + \frac{\tau_i^2}{(\tau_{IC} - \tau_i)(T_2 - \tau_i)} e^{-t/\tau_i}] = n_b^* a_b(t) \tag{S4}$$

The parallel and perpendicular fluorescence signals from the superposition state $|\Psi(t)\rangle$ can be easily derived, [1]

$$S_{//} = n_c(t)[\frac{3}{5}(n_a^*\mu_a{}^2 + n_b^*\mu_b{}^2) + \frac{2}{5}\sqrt{n_a^* n_b^*}\mu_a\mu_b\cos(\Delta t)]f_c \quad \text{(S5)}$$

$$S_{\perp} = n_c(t)[\frac{1}{5}(n_a^*\mu_a{}^2 + n_b^*\mu_b{}^2) - \frac{1}{5}\sqrt{n_a^* n_b^*}\mu_a\mu_b\cos(\Delta t)]f_c \quad \text{(S6)}$$

Similarly, the parallel and perpendicular fluorescence signals from the ^1L_a and ^1L_b state, as well as the ^1L_a state that is transferred from the ^1L_b state have the following forms, [2]

$$P_{//} = \frac{3}{5}(n_a(t)\mu_a{}^2 f_a + n_b(t)\mu_b{}^2 f_b) + \frac{1}{5}n_{ba}(t)\mu_a{}^2 f_{ba} \quad \text{(S7)}$$

$$P_{\perp} = \frac{1}{5}(n_a(t)\mu_a{}^2 f_a + n_b(t)\mu_b{}^2 f_b) + \frac{2}{5}n_{ba}(t)\mu_a{}^2 f_{ba} \quad \text{(S8)}$$

Here μ_a and μ_b are the emission transition dipoles of the ^1L_a and ^1L_b states, and f_c, f_a, f_b and f_{ba} are the emission coefficients of the superposition state, the ^1L_a state, ^1L_b state and ^1L_a state that is transferred from ^1L_b state at a given wavelength, respectively. Δ is the angular frequency difference between the ^1L_a and ^1L_b states. Assuming the slow change of cos(Δt) in the short time of τ_{IC} and T_2, thus cos(Δt)≈1. Finally, the total parallel and perpendicular signals are as follows.

$$I_{//} = S_{//} + P_{//} = n_c(t)\mu_a{}^2[\frac{3}{5}(n_a^* + \alpha^2 n_b^*) + \frac{2}{5}\alpha\sqrt{n_a^* n_b^*}]f_c + \frac{3}{5}[n_a(t)f_a + \alpha^2 n_b(t)f_b] + \frac{1}{5}n_{ba}(t)f_{ba} \quad \text{(S9)}$$

$$I_{\perp} = S_{\perp} + P_{\perp} = n_c(t)\mu_a{}^2[\frac{1}{5}(n_a^* + \alpha^2 n_b^*) - \frac{1}{5}\alpha\sqrt{n_a^* n_b^*}]f_c + \frac{1}{5}[n_a(t)f_a + \alpha^2 n_b(t)f_b] + \frac{2}{5}n_{ba}(t)f_{ba} \quad \text{(S10)}$$

where $\alpha = \mu_b / \mu_a$. Furthermore, we define $N_a^0 = \frac{n_a^*}{n_b^*}$, $\beta_1 = \frac{f_a}{f_{ba}}$, $\beta_2 = \frac{f_b}{f_{ba}}$, $\beta_3 = \frac{f_c}{f_{ba}}$ and will get

$$r(t) = \frac{I_{//} - I_{\perp}}{I_{//} + 2I_{\perp}} = \frac{[2(N_a^0 + \alpha^2) + 3\alpha\sqrt{N_a^0}]c(t)\beta_3 + 2[N_a^0 a(t)\beta_1 + \alpha^2 b(t)\beta_2] - a_b(t)}{5[(N_a^0 + \alpha^2)c(t)\beta_3 + N_a^0 a(t)\beta_1 + \alpha^2 b(t)\beta_2 + a_b(t)]} \quad \text{(S11)}$$

When t=0, $c(t)$=1, $a(t)$=$b(t)$=$a_b(t)$=0 and the anisotropy can be simplified as

$$r(0) = \frac{2}{5} + \frac{3\alpha\sqrt{N_a^0}}{5(N_a^0 + \alpha^2)} \quad \text{(S12)}$$

Assuming $\alpha = \mu_b / \mu_a = 1, N_a^0 = n_a^* / n_b^* = 1$, we will get $r(0)$=0.7, which is consistent with ref. 1. As for tryptophan, the typical values of α and N_a^0 are 0.455 and 1.2 (at 290-nm excitation), thus we get $r(0)$=0.61. However, it is important to note that the experimental value appears much smaller than the calculated value of 0.61 due to the actual temporal resolution.

When $t \gg T_2, \tau_{IC}$, $c(t)$=$b(t)$=0, $a(t)$≈$a_b(t)$ and the anisotropy is

$$r(t) = \frac{2N_a^0\beta_1 - 1}{5(N_a^0\beta_1 + 1)} \tag{S13}$$

Therefore, the plateau value of $r(t)$ after the coherence dephasing and CI dynamics is directly related to $N_a^0\beta_1$, *i.e.*, $\frac{n_a^* f_a}{n_b^* f_{ba}}$. If f_a=f_{ba} and $\frac{n_a^*}{n_b^*} = 1.2$, r=0.127 for the initial plateau.

(2) Parallel model

In this model, the key assumption is that the population flow is not necessary to start after dephasing. Instead, the CI dynamics and the dephasing process occur simultaneously. The time-dependent population of the ^1L_a state, ^1L_b state and ^1L_a state that is transferred from ^1L_b state are

$$n_a(t) = n_a^* \sum_i a_i e^{-t/\tau_i} = n_a^* a(t), \ \sum_i a_i = 1 \tag{S14}$$

$$n_b(t) = n_b^* e^{-t/\tau_{IC}} = n_b^* b(t) \tag{S15}$$

$$n_{ba}(t) = n_b^* \sum_i a_i \frac{\tau_i}{\tau_i - \tau_{IC}} (e^{-t/\tau_i} - e^{-t/\tau_{IC}}) = n_b^* a_b(t) \tag{S16}$$

Meantime, there is an interference term in the fluorescence emission

$$I_{in}(t) = \sqrt{n_a^* n_a^*} \sum_i a_i e^{-t(\frac{1}{2\tau_{IC}} + \frac{1}{T_2} + \frac{1}{2\tau_i})} \cos(\Delta t) \approx \sqrt{n_a^* n_a^*} \sum_i a_i e^{-t(\frac{1}{2\tau_{IC}} + \frac{1}{T_2} + \frac{1}{2\tau_i})} = \sqrt{n_a^* n_a^*} l(t) \tag{S17}$$

Similarly, we can get

$$I_{//} = \frac{3}{5}[n_a(t) f_a + \alpha^2 n_b(t) f_b] + \frac{2}{5}\alpha\sqrt{n_a^* n_b^*} l(t) \sqrt{f_a f_b} + \frac{1}{5} n_{ba}(t) f_{ba} \tag{S18}$$

$$I_{\perp} = \frac{1}{5}[n_a(t) f_a + \alpha^2 n_b(t) f_b] - \frac{1}{5}\alpha\sqrt{n_a^* n_b^*} l(t) \sqrt{f_a f_b} + \frac{2}{5} n_{ba}(t) f_{ba} \tag{S19}$$

$$r(t) = \frac{I_{//} - I_{\perp}}{I_{//} + 2I_{\perp}} = \frac{2[N_a^0 a(t)\beta_1 + \alpha^2 b(t)\beta_2] + 3\alpha\sqrt{N_a^0 \beta_1 \beta_2} l(t) - a_b(t)}{5[N_a^0 a(t)\beta_1 + \alpha^2 b(t)\beta_2 + a_b(t)]} \tag{S20}$$

The definitions of $f_a, f_b, f_{ba}, \alpha, \beta_1, \beta_2$ are the same as defined in the sequential model.

When t=0, $a(t)$=$b(t)$=l(t)=1, $a_b(t)$=0 and thus we have

$$r(0) = \frac{2}{5} + \frac{3\alpha\sqrt{N_a^0\beta_1\beta_2}}{5(N_a^0\beta_1 + \alpha^2\beta_2)} \tag{S21}$$

Assuming β_1=β_2=1, r(0) will be the same as eq. S12 in the sequential model.

When $t \gg T_2, \tau_{IC}$, $b(t)$=l(t)=0, $a(t)$≈$a_b(t)$ and

$$r(t) = \frac{2N_a^0\beta_1 - 1}{5(N_a^0\beta_1 + 1)} \tag{S22}$$

is the same as eq. S13 in the sequential model.

We simulated our experimental data with both models and found that the sequential model fits the data better while the parallel model has some deviation from the measured results. In Figure S1, the simulated anisotropies with the two models are compared with the experimental data for the mutant F30W gated at 310 nm. As shown clearly, the sequential model fits better than the parallel models. Therefore, the results presented in the main text are obtained from the simulations with the sequential model.

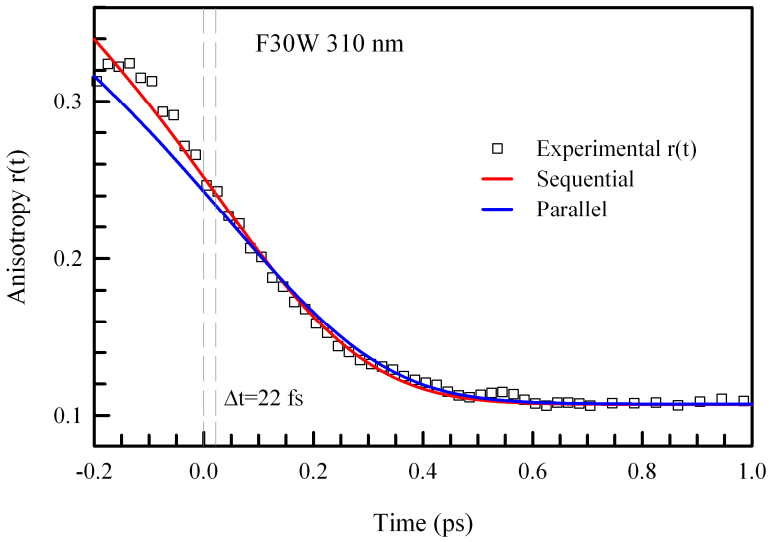

Figure S1. Simulated anisotropies of the mutant F30W at 310 nm with parallel (blue) and sequential (red) models compared with experimental data (squares).

References

[1] Wynne, K.; Hochstrasser, R. M. *J. Raman Spectrosc.* **1995**, *26, 561-569.*

[2] Bräm, O.; Oskouei, A. A.; Tortschanoff, A.; van Mourik, F.; Madrid, M.; Echave, J.; Cannizzo, A.; Chergui, M. *J. Phys. Chem. A* **2010***, 114, 9034-9042.*